

Minimal-Knowledge Assumptions in Digital Still Camera Characterization I.: Uniform Distribution, Toeplitz Correlation

J A Stephen Viggiano
RIT Research Corporation
Rochester, NY

Introduction

Scanners are usually presented with one medium (*e.g.*, a particular color transparency material) at a time. The non-arbitrary nature of the spectra presented to the device may be exploited in the characterization process, so that profiles with greater accuracy for a particular medium may be generated. It is customary to have a separate characterization for each medium type. Users of these devices may be familiar with this feature, often presented in the form of a menu in the scanner's user interface. Each characterization is intended to produce optimal results for that particular type of medium.

Digital still cameras (DSCs), unlike scanners, are presented with arbitrary radiance spectra. Accordingly, it is appropriate to make fewer assumptions about the spectra being captured. Techniques for DSC characterization based on the statistics of an infinite set of spectra would therefore be more appropriate than those based on a finite characterization set.

ISO Working Draft 17321-1 [1] provides for two different approaches to DSC characterization: one based upon measuring the camera's spectral sensitivities; the other based upon measuring patches in a color chart and relating the known tristimulus values of each patch to the corresponding camera output. The current working draft focuses on the stimuli, methodology, and test procedures for both approaches; presumably future versions will discuss analysis and computations. This paper addresses an analysis strategy for the first approach, using statistics of the spectra.

In the past, those possessing the spectral sensitivities of a color capture device could, in the absence of information on the spectra presented to the device, simply regress the spectral tristimulus values of the desired viewing illuminant onto the device's spectral sensitivities (weighted by the taking illuminant) to obtain a 3x3 linear RGB to XYZ transformation matrix. As lucidly pointed out by Finlayson and Drew, [2] this tacitly assumes that the relative radiance spectra presented to the device are bounded between -1 and 1, which admits physically impossible spectra. They suggested an approach, termed "Maximum Ignorance With Positivity," wherein the relative spectral radiances are bounded between zero and unity, as is the case in the real world. They demonstrated an improvement in accuracy after incorporating this constraint.

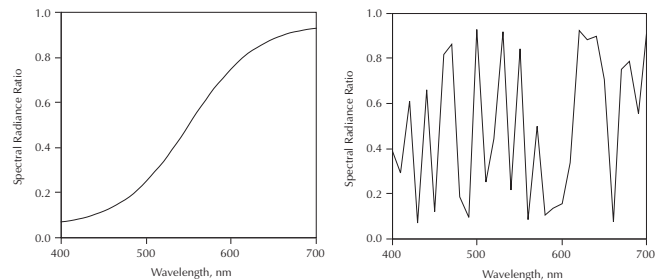


Figure 1.

In (a), at left, the relative radiances progress smoothly from one end of the spectrum to the other. In (b), at right, many jumps are observed. Which spectrum is more likely to be encountered in real life?

Finlayson and Drew assumed that the relative spectral radiances were uncorrelated with a uniform statistical distribution. In this paper, we explore effect on accuracy of permitting the spectral radiances to be correlated. In future papers, we plan to investigate the effect of other conditions, such as statistical distribution and constant mean. Because they incorporate slightly more information than Maximum Ignorance, we refer to these techniques as "Minimal Knowledge."

Figure 1 shows two spectra. Both spectra consist of the same values, but that are arranged differently. In the spectrum on the left, a smooth transition from low to high is exhibited, and the correlation between spectral radiances 10nm apart is 0.998. In the spectrum on the right, many jumps up and down are exhibited, and the correlation between spectral radiances 10mm apart is -0.082. Both spectra are given equal weight by Finlayson and Drew. We argue that the spectrum on the left is more representative of those encountered in practice than the one on the right, and should be given greater weight in a DSC or scanner characterization scheme.

Symbols and Terminology

We adopt the convention of bold for vectors (lower case) and matrices (upper case).

n_w The number of wavelengths in the sampled spectra, *e.g.*, 31.

n_s The number of spectra in a characterization or evaluation suite; *e.g.*, 24 for the Macbeth Color Checker.

- B** Matrix containing the relative radiance spectra, $n_s \times n_w$. Each row contains a spectrum; each column represents a particular wavelength.
- D** Device Spectral Sensitivities, $n_w \times 3$.
- T** Color Matching Functions, $n_w \times 3$.
- S_t** (Taking SPD) Diagonal matrix containing the taking illuminant, $n_w \times n_w$. Zeros off-diagonal.
- S_v** (Viewing SPD) Diagonal matrix containing the viewing illuminant, $n_w \times n_w$. Zeros off-diagonal.
- C** Camera linear response, $n_s \times 3$. Each row contains an RGB triplet.
- X** Tristimulus values of the spectra contained in **B**, $n_s \times 3$. Each row contains an XYZ triplet.
- A** Matrix to (approximately) transform linear camera RGB into tristimulus values, 3×3 .
- μ_i Mean of the relative spectral radiance at wavelength i .
- σ_i Standard Deviation of the relative spectral radiance at wavelength i .
- ρ_{ij} Correlation between relative spectral radiances at wavelengths i and j .
- b_{ij} An element of the matrix $\mathbf{B}^t \mathbf{B}$.

Mathematical Foundation

The tristimulus values of a collection of n_s spectra, contained in matrix **B**, as viewed by an observer whose color matching functions are contained in matrix **T** under an illuminant whose spectral power distribution is on the diagonal of matrix **S_v**, is:

$$\mathbf{X} = \mathbf{B} \cdot \mathbf{S}_v \cdot \mathbf{T} \quad (1)$$

(Note that one may use weights for tristimulus integration, such as those provided in ASTM E308, in place of the matrix product $\mathbf{S}_v \cdot \mathbf{T}$.)

Similarly, the linear camera RGB evoked by the same spectra, when captured under taking illuminant **S_t** by a camera with spectral sensitivities contained in **D**, will be:

$$\mathbf{C} = \mathbf{B} \cdot \mathbf{S}_t \cdot \mathbf{D} \quad (2)$$

We seek a matrix, **A**, which provides the “best” transformation from the linear camera RGBs contained in **C** to the tristimulus values contained in **X**. Ordinary linear least squares is a popular criterion; it provides the solution in closed form:

$$\begin{aligned} \mathbf{A} &= (\mathbf{C}^t \cdot \mathbf{C})^{-1} \cdot \mathbf{C}^t \cdot \mathbf{X} \\ &= (\mathbf{D}^t \cdot \mathbf{S}_t \cdot \mathbf{B}^t \cdot \mathbf{B} \cdot \mathbf{S}_t \cdot \mathbf{D})^{-1} \cdot \mathbf{D}^t \cdot \mathbf{S}_t \cdot \mathbf{B}^t \cdot \mathbf{B} \cdot \mathbf{S}_v \cdot \mathbf{T} \end{aligned} \quad (3)$$

Note that the matrix **B** enters Equation 3 only in the form of its own inner product, $\mathbf{B}^t \mathbf{B}$. Thus, it is only neces-

sary to specify this inner product matrix. The implicit manner in which **B** enters Equation (3) permits us to focus on how the matrix $\mathbf{B}^t \mathbf{B}$ is populated, rather than the specific spectra from which it is produced. As indicated earlier, we do this based on the statistics of the spectra:

$$b_{ij} = \rho_{ij} \cdot \sigma_i \cdot \sigma_j + \mu_i \cdot \mu_j \quad (4)$$

Because the correlation of a random variable with itself is unity, the diagonal elements will be:

$$b_{ii} = \sigma_i^2 + \mu_i^2 \quad (5)$$

For the uniform distribution on $[0, 1]$, $\mu = 0.5$ and $\sigma^2 = 1/12$. Substituting these values into Equations (4) and (5) yields, for uncorrelated spectral radiances, values of $1/3$ on the diagonal and $1/4$ off the diagonal, in agreement with Finlayson and Drew’s $\mathbf{B}^t \mathbf{B}$ matrix.

In this paper, we relax the assumption of uncorrelated spectra, giving greater weight to the spectrum to the left of Figure 1, and less weight to the spectrum to the right. Thus, the off-diagonal elements of $\mathbf{B}^t \mathbf{B}$ will not necessarily be $1/4$, but shall assume values between $1/3$ and $1/4$. In future papers, we will investigate the relaxation of additional assumptions.

Toeplitz Matrices and Correlation as a Function of Separation

While the only restrictions on a correlation matrix of real data are that it be Gramian (*i.e.*, symmetric and positive semi-definite) and contain unities on the diagonal, we impose a further constraint. In this paper, we consider only correlation matrices of Toeplitz form. Toeplitz correlation matrices, which arise in time-series analysis, are defined by their first column, and contain a series of bands either side of the main diagonal. All elements in a band are the same. The correlation between spectral radiances at two different wavelengths is, with such a matrix, a function of the distance between their wavelengths.

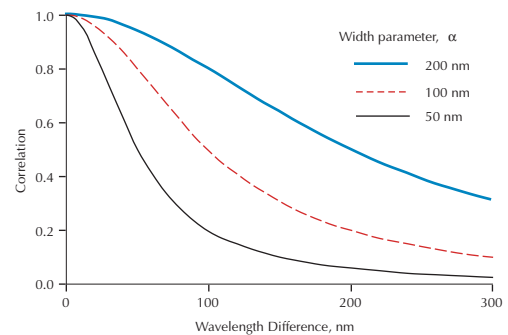


Figure 2. Correlation as a function of wavelength difference is illustrated for three different values of width parameter, α .

The correlation coefficient ρ_{ij} is assumed here to, in general, be close to unity when wavelengths i and j are very close, then gradually fall off as the separation between them increases. We arbitrarily use the following form:

$$\rho_{ij} = \frac{\alpha^2}{\alpha^2 + (\lambda_i - \lambda_j)^2} \quad (6)$$

which is the Cauchy function in $\lambda_i - \lambda_j$. The parameter α is the wavelength interval at which the correlation will be one-half. This function is plotted for several values of α in Figure 2. In the limit as α approaches zero, the function approaches a delta function, allowing non-zero correlations only when the two wavelengths are equal.

A mesh diagram of a correlation matrix with width parameter $\alpha = 100\text{nm}$ appears as Figure 3. The maximum correlation, along the main diagonal, is 1.0. The minimum in the plot, the correlation between radiances at 400nm and 700nm, is 0.10.

Experimental

The sensitivity spectrum (10 nm increments, between 400 and 700 nm) of a monochrome DSC was provided by Dr Francisco Imai of the Munsell Color Science Laboratory at RIT. We constructed a device sensitivity matrix \mathbf{D} using this information and the transmission spectra of Wratten 26 (Red), 58 (Green), and 47 (Blue) filters. These sensitivities are plotted in Figure 4. Our camera simulator consisted of this matrix and the spectral power distribution of the D65 taking illuminant. The camera simulator was exercised for radiance ratio spectra of 170 objects, provided by Vhrel and Trussel [3] of North Carolina State University, producing an RGB triplet for each. In addition, the tristimulus values (D65 viewing illuminant, 1931 observer) of each spectrum were computed in accordance with the recommendations of ASTM E308. These linear RGB and XYZ triplets were later used for assessment of goodness of fit.

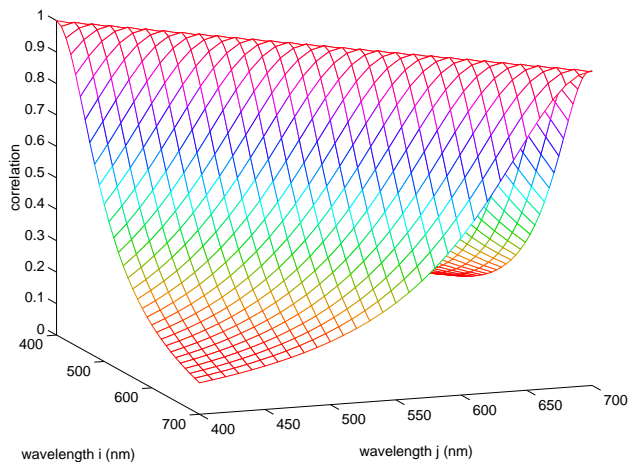


Figure 3. The correlation matrix, for width parameter $\alpha = 100\text{nm}$. The correlation between the radiances at 400nm and 700nm is 0.10.

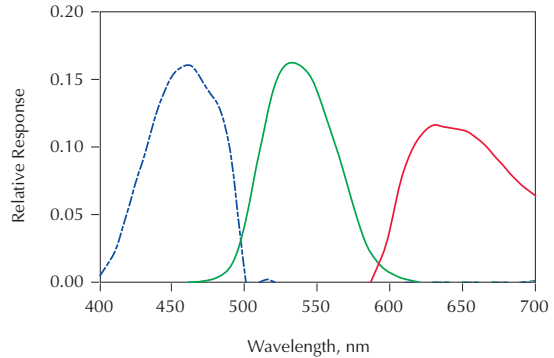


Figure 4. The spectral sensitivities of the monochrome camera with tri-color filters are plotted.

We also synthesized camera sensitivities using triangular sensitivity functions. The peaks were arbitrarily placed at 435nm, 545nm, and 645nm, or roughly near the centers of the Blue, Green, and Red portions of the spectrum. Full widths at half heights of 50, 60, and 70 nanometers were exercised. The sensitivity curves for the 50nm bandwidth set are illustrated in Figure 5; the others appear similar (but broader in bandwidth).

Assuming a viewing illuminant of D65 as well, and the 1931 observer, we computed the transformation matrix \mathbf{A} for various levels of the parameter α . Specifically, we used 0nm (which is Maximum Ignorance with Positivity) through 200 nm, at 50nm intervals. We also computed the matrix for a scalar $\mathbf{B}^t\mathbf{B}$ matrix (*i.e.*, Maximum Ignorance without positivity). The matrices were applied to the RGB triplets generated by the camera simulator, and compared to the XYZ tristimulus values obtained from the spectra by tristimulus integration. Our comparison criterion was ΔE^*_{ab} . The quantiles of the ΔE^* distributions were computed in accordance with the recommendations of CIE TC8-02. [4]

Our hypothesis is that an α greater than zero will produce smaller values of ΔE^* than those produced by an α of zero (Maximum Ignorance with Positivity) or with a diagonal $\mathbf{B}^t\mathbf{B}$ matrix (Maximum Ignorance without Positivity). We further hypothesize that distributions of ΔE^* will be

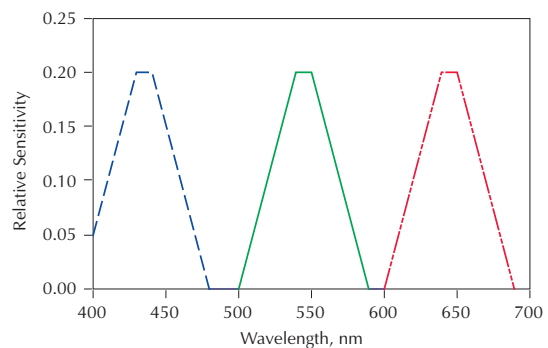


Figure 5. The sensitivities of one of the synthetic cameras (50nm bandwidth) are plotted. Other synthetic sensitivities were used in this study; they had 60nm and 70nm bandwidths.

| Quantile | α : | 0* | 0† | 50 | 100 | 150 | 200 |
|-----------------|------------|-------|-------|-------|-------|-------|-------|
| Min: | | 1.26 | 0.42 | 0.12 | 0.14 | 0.15 | 0.07 |
| 0.1 | | 3.25 | 1.02 | 0.65 | 0.64 | 0.47 | 0.36 |
| 0.2 | | 5.12 | 2.11 | 1.14 | 1.10 | 0.96 | 0.77 |
| 0.3 | | 5.90 | 2.90 | 1.62 | 1.98 | 1.87 | 1.62 |
| 0.4 | | 6.38 | 3.68 | 2.74 | 2.72 | 2.47 | 2.08 |
| 0.5 | | 7.08 | 4.50 | 3.47 | 3.23 | 3.16 | 2.76 |
| 0.6 | | 8.37 | 4.88 | 4.33 | 3.94 | 3.69 | 3.02 |
| 0.7 | | 9.92 | 5.81 | 5.03 | 4.87 | 4.06 | 3.50 |
| 0.8 | | 11.69 | 7.30 | 5.82 | 5.30 | 4.69 | 4.86 |
| 0.9 | | 14.51 | 10.17 | 7.08 | 6.55 | 6.52 | 6.56 |
| 0.95 | | 17.29 | 13.13 | 10.31 | 9.31 | 8.29 | 9.79 |
| Max: | | 20.51 | 21.73 | 21.84 | 25.55 | 29.49 | 31.87 |
| Mean: | | 8.31 | 5.09 | 3.94 | 3.81 | 3.63 | 3.48 |
| Std Dev: | | 4.25 | 4.03 | 3.56 | 3.60 | 3.81 | 4.12 |

Table 1. Selected quantiles of ΔE^* , for Maximum Ignorance (with and without Positivity), and new method with $\alpha = 50\text{nm}$ [50nm] 200nm, for three monochrome camera with tricolor filters. Within a row, the smaller the quantile, the better.

*Maximum Ignorance. † Maximum Ignorance with Positivity.

lower for non-zero α values than for α of zero (Maximum Ignorance with Positivity). While it would be nice to test all positive values of α , from a practical standpoint we must select one or two. Somewhat arbitrarily, we selected 50nm and 100 nm.

Results & Discussion

Monochrome Camera Results

The results for the monochrome camera with the red, green, and blue filters appear in Table 1, above. In addition to the mean and standard deviation of ΔE^* , selected quantiles also appear, as recommended by CIE TC8-02. The results for Maximum Ignorance (both with and without Positivity) are also included.

Although a monotonic downward trend is observed with the mean ΔE^* with respect to α , we see that there is an upward trend with regard to the maximum. The downward monotonic trend is also observed for the minimum, and all quantiles up to and including 0.7. For quantiles 0.8, 0.9, and 0.95, the minimum occurs at $\alpha = 150$ nm. The value of $\alpha = 150$ nm would thus be a reasonable value to select for this particular set of spectral sensitivities.

The one-sided Smirnov test was used to test the hypothesis that the ΔE^* s were larger when Maximum Ignorance with Positivity was used, versus using correlated spectra with α s of 50nm and 100nm, respectively. This statistic is based on the sample frequency ogives (cumulative histograms) being compared. In this case, it is the maximum difference, in probability, by which the Maximum Ignorance with Positivity ogive is exceeded by that of the

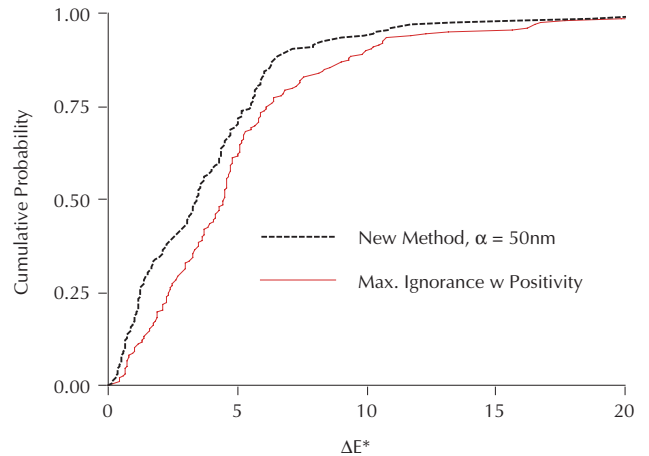


Figure 6. The frequency ogives of ΔE^* for the monochrome camera with tricolor filters are shown for matrices computed using Maximum Ignorance with Positivity (thin solid), and using the new technique with $\alpha = 50\text{nm}$ (thick dashed). The former curve is, in general, below the latter, indicating a trend for smaller ΔE^* s to come from the new method. A higher curve indicates smaller ΔE^* s.

ogive produced with an α of either 50nm or 100nm. This was 0.1706 for $\alpha = 50\text{nm}$ (significant at 0.05 level), and 0.2059 for $\alpha = 100\text{nm}$ (significant at 0.01 level). (These correspond to lags of 29 and 35 samples, respectively.)

The ogives for Maximum Ignorance with Positivity and for the new technique with $\alpha = 50\text{nm}$ appear in Figure 6. (One may produce frequency histograms by smoothing and differentiating these ogives.) Note that the ogive of the ΔE^* s from the Maximum Ignorance with Positivity is, in general, below that of the ogive of the ΔE^* s produced by the new method. This indicates that smaller ΔE^* s are produced, in general, using the new method.

Synthetic Camera Results

Similar trends were observed for the synthetic sensitivities, though the optimal values (in terms of smallest 95th percentile) of α were lower: 35.2nm for the sensitivities with 50nm bandwidths; 60.2nm for the sensitivities with 60nm bandwidths, and 68.5nm for the sensitivities with 70nm bandwidths. Rather than present the extensive report for the synthetic cameras with many different values of α , as was done for the monochrome camera with tricolor filters in Table 1, Table 2 contains the comparison of the selected quantiles of the ΔE^* s for Maximum Ignorance with Positivity and for the new technique with width parameter $\alpha = 50\text{nm}$, for the three synthetic cameras. An improvement over the prior art is apparent for the synthetic cameras with bandwidths of 50nm and 60nm at all quantiles, as well as the maxima. The results for the synthetic camera with the 70nm bandwidth are mixed, with the means essentially equal.

The Smirnov tests also yielded similar results: the results are summarized in Table 3. As before, the new method yielded distributions of ΔE^* which tended to pro-

Synthetic Camera Bandwidth:

| Quantile | α : | 50nm | | 60nm | | 70nm | |
|-----------------|------------|-------|-------|-------|-------|-------|-------|
| | | 0* | 50 | 0* | 50 | 0* | 50 |
| Min: | | 0.28 | 0.14 | 0.10 | 0.10 | 0.12 | 0.12 |
| 0.1 | | 2.06 | 0.86 | 1.57 | 0.91 | 1.46 | 0.98 |
| 0.2 | | 3.68 | 1.44 | 2.63 | 1.74 | 2.24 | 1.70 |
| 0.3 | | 4.33 | 1.99 | 3.04 | 2.43 | 2.85 | 2.56 |
| 0.4 | | 4.98 | 2.71 | 3.33 | 3.10 | 3.50 | 3.27 |
| 0.5 | | 5.60 | 3.42 | 4.10 | 3.98 | 3.71 | 4.17 |
| 0.6 | | 6.99 | 4.63 | 4.94 | 4.95 | 4.17 | 5.09 |
| 0.7 | | 7.71 | 5.33 | 6.03 | 5.91 | 4.89 | 6.12 |
| 0.8 | | 9.45 | 6.29 | 7.39 | 6.72 | 6.65 | 6.79 |
| 0.9 | | 15.35 | 9.60 | 11.56 | 8.39 | 9.95 | 8.11 |
| 0.95 | | 20.87 | 15.86 | 16.95 | 13.85 | 13.28 | 11.86 |
| Max: | | 45.48 | 25.60 | 32.50 | 29.87 | 19.90 | 33.29 |
| Mean: | | 7.65 | 4.61 | 5.69 | 4.74 | 4.80 | 4.79 |
| Std Dev: | | 6.81 | 4.51 | 5.10 | 4.21 | 3.73 | 4.21 |

Table 2. Selected quantiles of ΔE^* , for Maximum Ignorance with Positivity, and new method with $\alpha = 50\text{nm}$, for three synthetic camera sensitivities. *Maximum Ignorance with positivity.

duce smaller values of ΔE^* than with Maximum Ignorance with Positivity. The results for the 50nm bandwidth camera were most striking, significant even at the 0.001 level. The results for the camera with the 70nm bandwidth sensitivities were not statistically significant at the 0.05 level.

Conclusions

A new technique for computing 3x3 matrices for DSC characterization has been described. It is a generalization of the Maximum Ignorance with Positivity method proposed by Finlayson and Drew, and, like that method, is based on the statistics of an infinite set of characterization spectra (rather than on a specific finite set). These techniques are arguably important for DSCs, which are presented with arbitrary spectra. Unlike Maximum Ignorance with Positivity, however, the new method admits spectra which have positive correlation between radiances at different wavelengths. The correlation between two spectral radiances is taken as a function of the difference of their wavelengths. This produces a correlation matrix in Toeplitz form.

Because the assumptions regarding the spectra in the characterization set are modest and may be compactly described (here, by one parameter), we refer to the new method as “Minimal Knowledge.”

The new technique demonstrated better performance (relative to Maximum Ignorance with Positivity) in terms of average ΔE^* , as well as all percentiles up to and including the 95th for positive values of the width parameter α up to 200nm, for three out of four cameras when the two tech-

Table 3: Smirnov Statistics

Camera: 50nm Bandwidth (optimal $\alpha = 35.2\text{nm}$)
 MIWP vs $\alpha = 50\text{nm}$: 0.3471 †
 MIWP vs $\alpha = 100\text{nm}$: 0.2701 †

Camera: 60nm Bandwidth (optimal $\alpha = 60.2\text{nm}$)
 MIWP vs $\alpha = 50\text{nm}$: 0.1588 *
 MIWP vs $\alpha = 100\text{nm}$: 0.1588 *

Camera: 70nm Bandwidth (optimal $\alpha = 68.5\text{nm}$)
 MIWP vs $\alpha = 50\text{nm}$: 0.1353
 MIWP vs $\alpha = 100\text{nm}$: 0.1412

MIWP: Maximum Ignorance with Positivity.

† Significant at 0.001 level.

* Significant at 0.05 level.

niques were compared using a standard comparison suite of 170 reflectance spectra.

Literature Cited

1. *Graphic technology and photography — Colour characterisation of digital still cameras (DSCs) — Part 1: Stimuli, metrology, and test procedures (ISO/WD 17321-1)*, August, 2000. Available online at: http://www.pima.net/standards/iso/tc42/WG20/N4591_WD17321-1_v1.PDF
2. Finlayson, Graham D., and Mark S. Drew, The maximum ignorance assumption with positivity. *Final Program and Proceedings of the IS&T/SID Fourth Color Imaging Conference*, 1996, p. 202 - 205.
3. Available online at <ftp://ftp.eos.ncsu.edu/pub/spectra/objects.spectra.10.Z>.
4. CIE TC8-02, *Methods to Derive Colour Differences for Images* (draft version 0.4), October, 2000. Available online at: <http://www.colour.org/tc8-02/cietc802v04.pdf>

Biography

J A STEPHEN VIGGIANO is Principal Scientist at the RIT Research Corporation, where he provides industry with solutions to problems in digital color image processing, color calibration and modeling, and tone reproduction. Steve is also a member of the graduate faculty of the School of Printing Management and Sciences at RIT, where he teaches courses in image reproduction theory, printing inks, paper, research methods, and color.

Professor Viggiano holds an AB degree in Mathematics from Thomas Edison College, and Master's Degrees from RIT in Printing Technology and Mathematical Statistics. He is a member of CIE TC8-02 (Color Differences in Images, for which he authored the section on statistics) and TC8-03 (Gamut Mapping).